Efficiency of the improved algorithm for controlling electrical and process modes of the modular-type electric arc furnace

A. A. Nikolaev, *Cand. Eng., Head of the Dept. of Automatic Electric Drive and Mechatronics* [1], *e-mail: aa.nikolaev@magtu.ru;*
P. G. Tulupov, *Cand. Eng., Associate Prof., Dept. of Automatic Electric Drive and Mechatronics* [1], *e-mail: tulupov.pg@mail.ru;*
M. V. Bulanov, *Cand. Eng., Associate Prof., Dept. of Automatic Electric Drive and Mechatronics* [1], *e-mail: bulanov.m.v@gmail.com;*
P. I. Svyatkin, *Postgraduate Student, Dept. of Automatic Electric Drive and Mechatronics* [1], *e-mail: svyatkin_p@mail.ru*

[1] *Nosov Magnitogorsk State Technical University, Magnitogorsk, Russia*

The paper describes the measures taken to improve energy efficiency of a 120-t modular-type electric arc furnace (EAF) and a furnace transformer with a rated capacity of 95 MVA. The first measure involved adjusting the automatic control system parameters for the electrical mode and electrode movement to reduce the static regulation error and improve dynamic performance of the control quality. The second measure was aimed at developing and studying an algorithm for automatic switching of the furnace transformer tap positions and operating curves using separate melting profiles for combinations of weight of the solid charge and hot metal. Upon implementation of these measures, we have assessed how they influenced the resulting energy efficiency of the EAF, and drawn the conclusions that the developed algorithms are universal and can be implemented on other modular-type arc steelmaking furnaces of different capacities.

Key words: modular-type electric arc furnace, electric arc, furnace transformer, electric arc current, slag coefficient
DOI: 10.17580/cisisr.2026.01.03

Introduction

Modern electrometallurgy is a promising and knowledge-intensive sector of the iron and steel industry. When revamping existing facilities and introducing new production capacities, the overwhelming majority of steel producers prefer to build electric steelmaking shops, where the process flow includes electric arc furnaces (EAF) and ladle furnaces (LF) [1–4]. In view of this, it is especially relevant to conduct research aimed at improving energy efficiency of furnaces by optimizing the automatic control system for the electrical mode and electrode movement.

The overwhelming majority of currently used control systems for the EAF and the LF are designed as a two-level structure. Following the melting profile, Level 2 sets the tap of furnace transformer N_{TR}, reactance coil N_R (if any) and operating curve number N_{OPCURV}. In most cases, a criterion for transferring from one melting stage to another one is specific power consumption W_{SP}. N_{TR} and N_R determine the shape of the electrical characteristic, showing the dependence between electric arc power P_{ARC} and arc length L_{ARC}, to adjust the amount of electric power supplied to the furnace. In its turn, N_{OPCURV} is responsible for the actual range of control parameter setpoints at Level 1 control system, determining an operating point on electrical characteristic $P_{ARC} = f(L_{ARC})$ and maintaining it by controlling the hydraulic drive for electrode movement [5–9].

To ensure maximum technical effect from optimization measures, it is necessary to take a set of measures to correct parameters and control algorithms both at Level 2 and Level 1. This approach was implemented on a 120-t modular-type electric arc furnace (95 MVA) operating at one of Russian iron and steel works. Thus, the purpose of the research is to study efficiency of the above measures as part of an improved algorithm for electrical mode control. A more detailed description of the EAF as the subject of study, and the optimization measures taken, will be provided below.

Specification of the EAF as the subject of study. Description of revealed functioning problems, influencing energy efficiency

The flexible modular-type the EAF under study functions in two main modes: 1) a conventional electric steel melting mode using the solid charge (scrap, HBI, pig iron, various scraps supplied by metallurgical shops) and step-by-step supply of hot metal amounting to 80 t during the melting process; 2) in a mode of the basic oxygen furnace, when a maximum share of hot metal achieves 85 % of a total charge weight.

For clarity, **Fig. 1** (*a*, *b*) present the EAF in the EAF shop, and a furnace drawing showing electrodes of phases 1–3, lances, which may also function as burners, carbon injectors and water-cooled panels.

During the operation of the EAF, the authors have identified the following problems, directly influencing energy efficiency of the furnace: 1) non-optimal parameters of the HI-REG electrical mode automatic control system, which result in controlling the complex with a significant

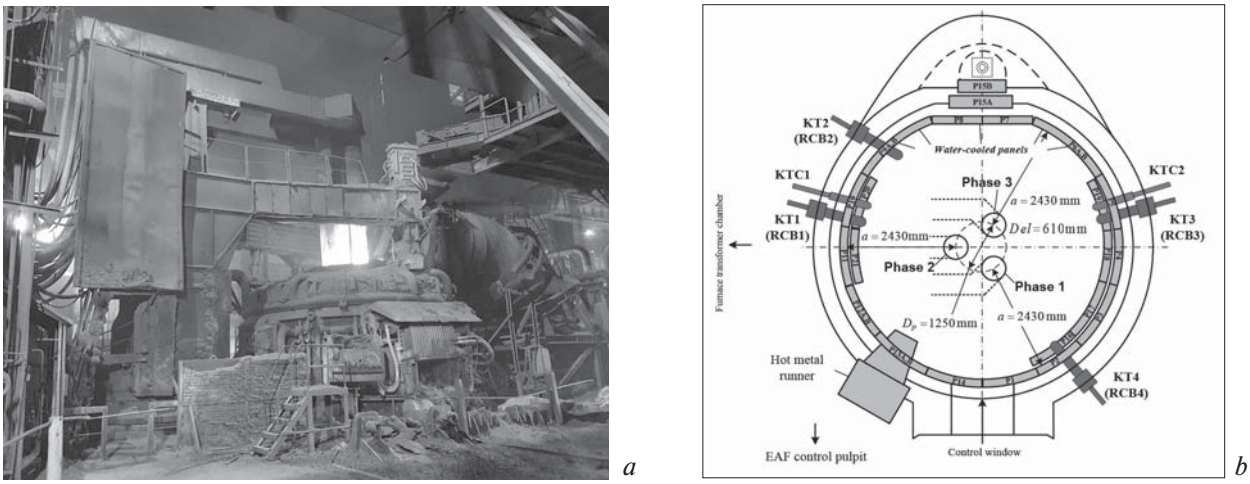

a *b*

Fig. 1. 120-t modular-type EAF (95 MVA) under study (*a*); the EAF drawing showing elec-trodes of phases 1–3, combined regenerative ceramic burners (KT, RCB), carbon injectors (KTC) and water-cooled panels (P1–P21) (*b*)

static error and slow transfer processes of control actions; 2) a complex structure of the EAF melting profiles and phase transition algorithms, as well as the inability to modify Level 2 ACS due to its closed architecture, have led to steelmakers using manual control of the EAF electrical modes, adjusting the on-load tap of the furnace transformer and the operating curve number, and visual monitoring of the metallurgical process during charge melting.

To settle the above problems, the authors optimized the HI-REG control system parameters and developed a system for automatic change-over of transformer taps and operating curves to apply individual melting profiles for different combinations of weight of the solid charge and hot metal. A more detailed description of the technical solutions used in the operation will be provided below.

Optimizing the HI-REG electrical mode control parameters

For clarity, a functional diagram of HI-REG is given in **Fig. 2**. A general description of the operation algorithm for this system is provided in the research paper [10].

The HI-REG parameters, namely adjustment factors K_A and K_I, were changed by applying the procedure developed in research [11]. A list of original and new parameters of K_A and K_I controllers in HI-REG of the EAF is given in **Table 1**. The use of new parameters for the HI-REG control system improved the regulation of the system's response to control actions, when changing the complex conductivity setpoint (**Fig. 3**) and, in turn, reduced the static error of the complex conductivity regulation from 17–24 % to 0.09–0.83%. Corresponding statistical performance indicators of the system at the original and new settings are summarized in **Table 2**.

Developing an algorithm for automatic changing of furnace transformer on-load taps and operating curves

To control the EAF electrical modes efficiently, we suggested 4 melting profiles: 1) profile 1 – cold start of the EAF after its repair without hot metal and using the charge and two additional charges; 2) profile 2 – a small share of hot metal (up to 40 t) and one additional charge; 3) profile 3 – with an average weight of hot metal (up to 75 t); 4) profile 4 – adding up to 90 t of hot metal. A main criterion for

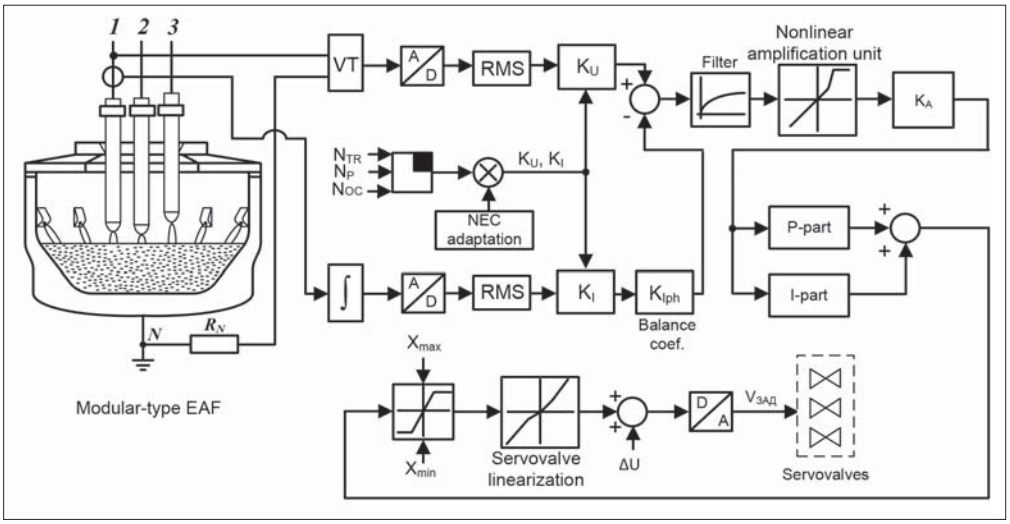

Fig. 2. A functional diagram of the HI-REG electrical mode control

Table 1. Original and new parameters K_I and K_A in HI-REG

On-load tap of the furnace transformer, N_{TR}	Original setting of HI-REG		New setting of HI-REG	
	K_I, per unit value	K_A, per unit value	K_I, per unit value	K_A, per unit value
1	1.535	2.658	1.685	2.918
2	1.446	2.504	1.587	2.749
3	1.356	2.349	1.489	2.580
4	1.312	2.272	1.391	2.410
5	1.267	2.195	1.294	2.241
6	1.223	2.118	1.245	2.156
7	1.178	2.041	1.196	2.071
8	1.134	1.964	1.147	1.986
9	1.089	1.886	1.098	1.901
10	1.045	1.809	1.049	1.817
11	1.000	1.732	1.000	1.732
12	0.000	0.000	0.000	0.000
13	0.886	1.535	0.973	1.685
14	0.835	1.446	0.916	1.587
15	0.783	1.356	0.860	1.489
16	0.757	1.312	0.803	1.391
17	0.732	1.267	0.747	1.293
18	0.706	1.223	0.719	1.245
19	0.680	1.178	0.690	1.196
20	0.655	1.134	0.662	1.147
21	0.629	1.089	0.634	1.098

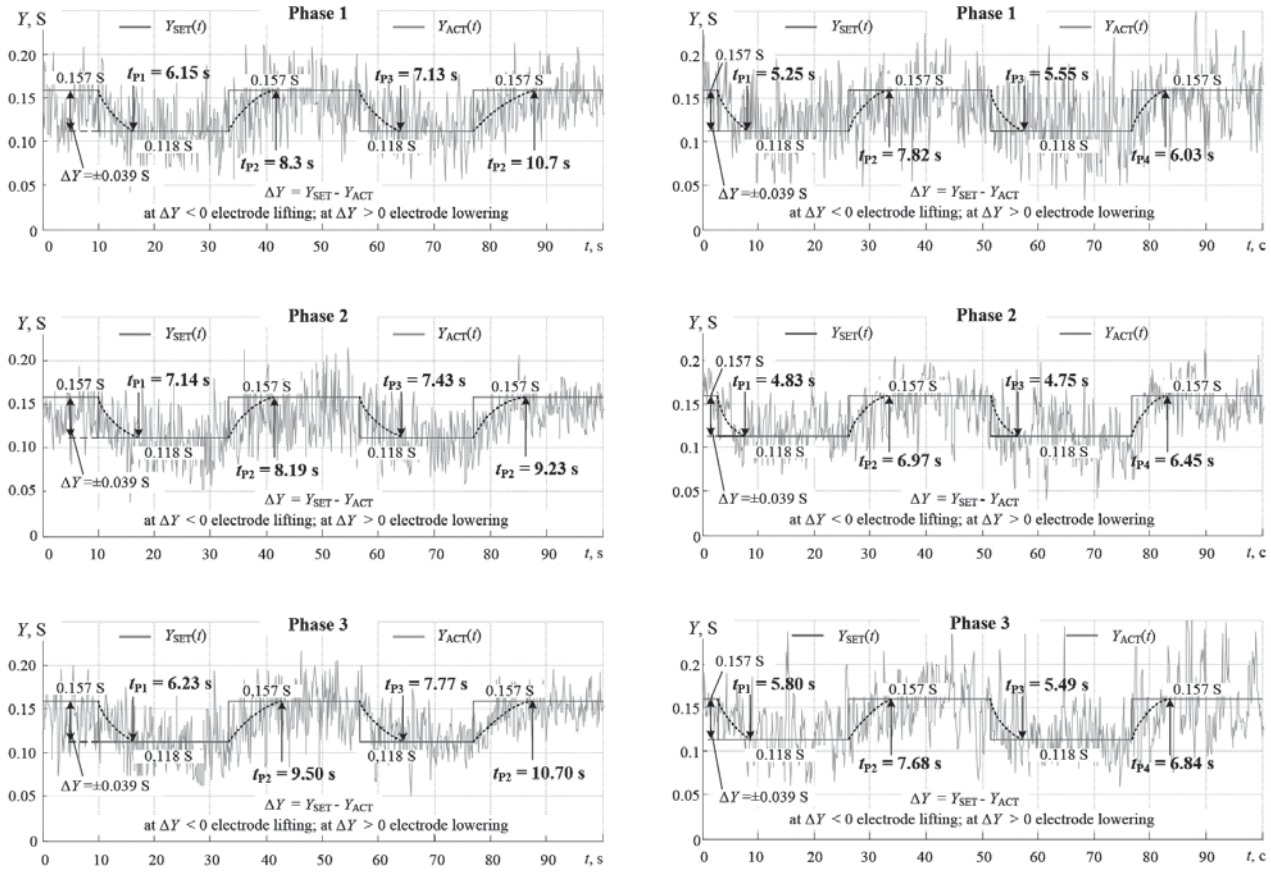

Fig. 3. Response of HI-REG to the tap change in the complex conductivity setpoint at the original settings of the system (*a*); the new settings of the system (*b*)

Table 2. HI-REG operation statistics at original and new settings

N_{TR}, N_R, N_{OC}	Measured current on the primary side of the furnace transformer				Recalculated current in HI-REG on the secondary side of the furnace transformer				$K_{T.CALC}$, per unit value	$K_{T.ACT}$, per unit value	δK_T, %
	$I_{1.1}$, A	$I_{1.2}$, A	$I_{1.3}$, A	$I_{1.AV}$, A	$I_{2.1}$, A	$I_{2.2}$, A	$I_{2.3}$, A	$I_{2.AV}$, A			
When using the **original settings** of the HI-REG control system											
16/4/3	871.90	895.60	885.80	884.43	54.08	53.49	52.65	53.41	60.39	51.20	**+17.94**
17/4/4	1049.0	1078.0	1067.0	1064.7	60.19	59.55	58.55	59.43	55.82	47.60	**+17.27**
19/4/5	1271.0	1308.0	1295.0	1291.3	65.97	65.29	64.10	65.12	50.43	44.00	**+14.61**
20/4/5	1202.0	1232.0	1220.0	1218.0	64.37	63.74	62.78	63.63	52.24	42.20	**+23.79**
When using the **new settings** of the HI-REG control system											
16/4/3	928.49	987.43	930.65	948.86	50.11	47.11	47.32	48.18	50.78	51.20	**–0.83**
17/4/4	1146.8	1177.0	1107.7	1143.8	55.68	52.20	54.60	54.16	47.35	47.60	**–0.52**
19/4/5	1332.0	1394.0	1335.0	1353.7	61.15	58.26	58.61	59.34	43.84	44.00	**–0.37**
20/4/5	1390.0	1428.0	1428.0	1415.3	60.27	60.10	58.86	59.74	42.21	42.20	**+0.03**

transferring from one combination NTR/NOPCURV to another one is specific electric power consumption calculated per weight of the solid charge (additional charge).

The algorithm for controlling the EAF electrical mode automatically switches the on-load tap of furnace transformer N_{TR} and operating curve number N_{OPCURV} according to the set tables of melting curves, where the N_{TR} / N_{OPCURV} combinations are selected depending on specific power consumption WSP calculated subject to weight of the charge and additional charges (if any). Every profile includes 3 tables for combinations N_{TR} / N_{OPCURV} for different melting stages of the charge and additional charges, and one table to select N_{TR} / N_{OPCURV} at the liquid steel refining stage. Every step of the process is set according to boundary values of specific power consumption $W_{SP.BOUND}$ compared with actual values WSP calculated independently during melting of every bucket. The formulae for calculating actual values W_{SP} are given below:

$$W_{SP.BUC1} = W_{ABS} / G_{BUC1}, \quad (1)$$

$$W_{SP.BUC2} = (W_{ABS} - W_{ABS.BUC1\Sigma}) / G_{BUC2}, \quad (2)$$

$$W_{SP.BUC3} = (W_{ABS} - (W_{ABS.BUC1\Sigma} + W_{ABS.BUC2\Sigma}) / G_{BUC3}, \quad (3)$$

$$W_{SP.REF} = (W_{ABS} - (W_{ABS.BUC1\Sigma} + W_{ABS.BUC2\Sigma} + W_{ABS.BUC2\Sigma}) / G_{BUC\Sigma}, \quad (4)$$

where W_{ABS} is a current value of the absolute power consumption from the beginning of the melting process [kW·h]; $W_{ABS.BUC1\Sigma}$ is power consumption for melting bucket 1 (the charge); $W_{ABS.BUC2\Sigma}$ is power consumption for melting bucket 2 (additional charge 1); $W_{ABS.BUC3\Sigma}$ is power consumption for melting bucket 3 (additional charge 2); G_{BUC1}, G_{BUC2}, G_{BUC2} is weight of bucket 1, 2 and 3 (the charge, additional charges 1 and 2); $G_{BUC\Sigma} = G_{BUC1}+G_{BUC2}+G_{BUC2}$ is total weight of the metal charge, excluding hot metal.

The developed melting profiles are given in **Fig. 4** and **5**. When adjusting the melting profiles, we applied the following approaches to control the EAF electrical modes:

1. A main profile among 4 existing ones is profile 3 used for 70% of heats, when hot metal weight ranges from 41 to 75 t. This category of heats is produced without any additional charge, as a rule, using one charging bucket. To intensify melting of the charge in a main melting period, the melting profile includes the N_{TR} / N_{OPCURV} combinations, ensuring the operation with long arcs and a higher electric arc radiation coefficient (N_{OPCURV} = 1 and 2). When melting wells in the charge is completed at lower taps N_{TR} = 15 and 17, an operator quickly switches to high taps N_{TR} = 19 and 21, while maintaining long electric arcs (N_{OPCURV} = 2 and 3). It should be noted that the applied algorithm for automatic control, time for transferring from combinations N_{TR} / N_{OPCURV} depends on charge weight G_{CHARGE} and set boundary specific power consumption W_{SP} for a specific process step. When charge weight G_{CHARGE} is high, the transition to higher taps N_{TR} occurs slower as opposed to the situation when charge weight G_{CHARGE} is less, which is attributed to a more continuous operation at lower taps N_{TR} for proper melting of wells. When reaching the end of melting the charge, arc length is automatically transferred to an average value (N_{OPCURV} = 4), when radiation is lower, power P_{ARC} and burning stability are higher. At a final stage of charge melting, a steelmaker manually switches over RCBs to the lance mode, the system transfers to the "Steel refining" profile table, when maximum tap N_{TR} = 21 is used in combination with operating curves N_{OPCURV} = 5 and 6 corresponding to a short arc mode, while achieving maximum heating rate coefficient and, consequently, molten bath heating speed.

2. The second most frequently used profile is profile 4 applied for heats containing much hot metal, namely from 76 to 90 t (from 12 % to 25 % of the total number of heats). This profile provides for the EAF electrical modes, when tap positions $N_{TR} \leq 18$, which is attributed to the need to limit the steel heating rate because of a longer decarburization stage during operation of RCBs in the blowing mode (to prevent unwanted overheating of the bath), as well as to prevent slag discharge from EAF during the charge melting.

3. The next most frequently used profile of profile 2 used in 10–20 % of heats, when hot metal weight is low (below 40 t). Profile 2 has similar combinations N_{TR} / N_{OPCURV} as in profile 3, but it uses higher boundary values of specific power consumption $W_{SP.BOUND}$, ensuring a longer operation with long arcs and slower transfer to higher values of N_{TR}. Electrical modes for the steel refining stage for profiles 2 and 3 are the same.

4. Melting profile 1 is rarely used (less than 5 % of heats) and applied for heats after repair of the EAF, without hot

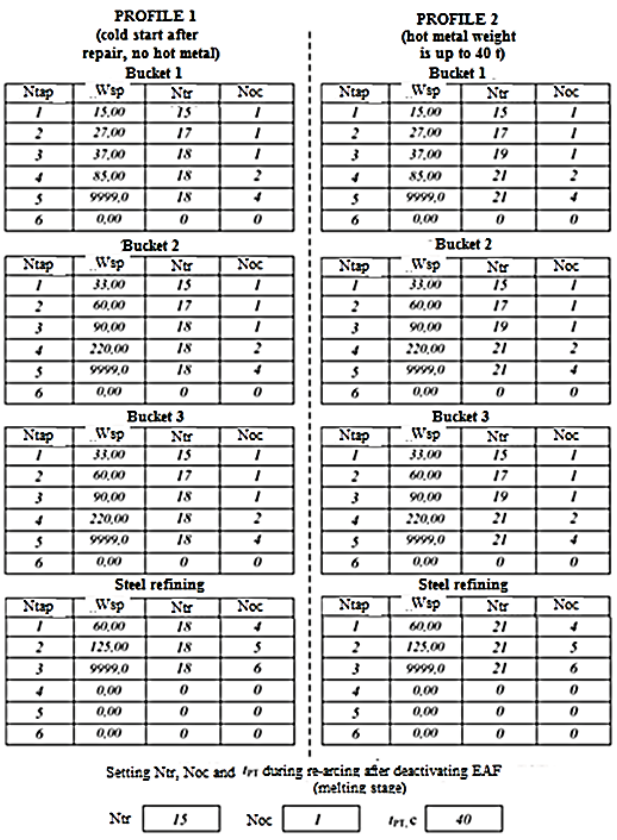

PROFILE 1
(cold start after repair, no hot metal)

Bucket 1

Ntap	Wsp	Ntr	Noc
1	15,00	15	1
2	27,00	17	1
3	37,00	18	1
4	85,00	18	2
5	9999,0	18	4
6	0,00	0	0

Bucket 2

Ntap	Wsp	Ntr	Noc
1	33,00	15	1
2	60,00	17	1
3	90,00	18	1
4	220,00	18	2
5	9999,0	18	4
6	0,00	0	0

Bucket 3

Ntap	Wsp	Ntr	Noc
1	33,00	15	1
2	60,00	17	1
3	90,00	18	1
4	220,00	18	2
5	9999,0	18	4
6	0,00	0	0

Steel refining

Ntap	Wsp	Ntr	Noc
1	60,00	18	4
2	125,00	18	5
3	9999,0	18	6
4	0,00	0	0
5	0,00	0	0
6	0,00	0	0

PROFILE 2
(hot metal weight is up to 40 t)

Bucket 1

Ntap	Wsp	Ntr	Noc
1	15,00	15	1
2	27,00	17	1
3	37,00	19	1
4	85,00	21	2
5	9999,0	21	4
6	0,00	0	0

Bucket 2

Ntap	Wsp	Ntr	Noc
1	33,00	15	1
2	60,00	17	1
3	90,00	19	1
4	220,00	21	2
5	9999,0	21	4
6	0,00	0	0

Bucket 3

Ntap	Wsp	Ntr	Noc
1	33,00	15	1
2	60,00	17	1
3	90,00	19	1
4	220,00	21	2
5	9999,0	21	4
6	0,00	0	0

Steel refining

Ntap	Wsp	Ntr	Noc
1	60,00	21	4
2	125,00	21	5
3	9999,0	21	6
4	0,00	0	0
5	0,00	0	0
6	0,00	0	0

Setting Ntr, Noc and t_{PT} during re-arcing after deactivating EAF (melting stage)

Ntr 15 Noc 1 t_{PT}, c 40

Fig. 4. Melting profiles 1, 2 for the algorithm applied to automatically change on-load taps of the furnace transformer and operating curves

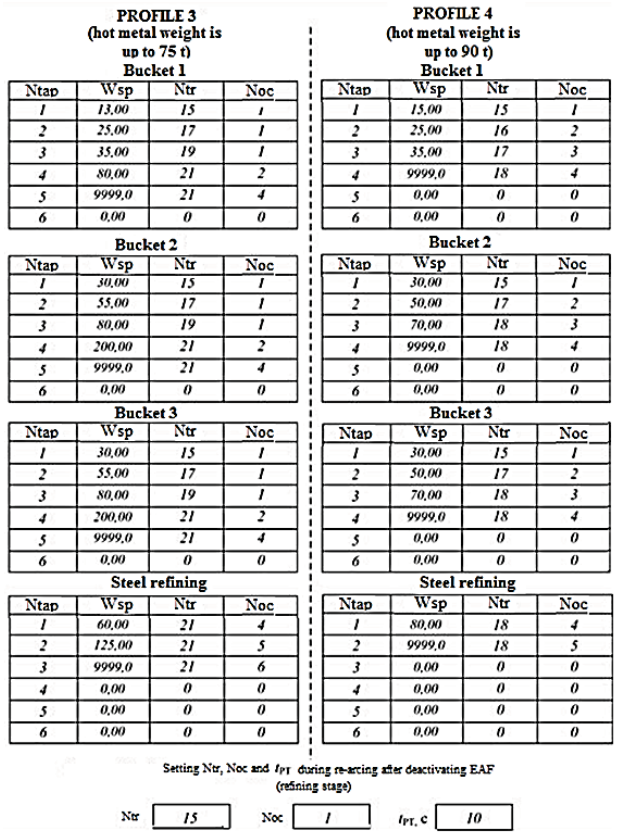

PROFILE 3
(hot metal weight is up to 75 t)

Bucket 1

Ntap	Wsp	Ntr	Noc
1	13,00	15	1
2	25,00	17	1
3	35,00	19	1
4	80,00	21	2
5	9999,0	21	4
6	0,00	0	0

Bucket 2

Ntap	Wsp	Ntr	Noc
1	30,00	15	1
2	55,00	17	1
3	80,00	19	1
4	200,00	21	2
5	9999,0	21	4
6	0,00	0	0

Bucket 3

Ntap	Wsp	Ntr	Noc
1	30,00	15	1
2	55,00	17	1
3	80,00	19	1
4	200,00	21	2
5	9999,0	21	4
6	0,00	0	0

Steel refining

Ntap	Wsp	Ntr	Noc
1	60,00	21	4
2	125,00	21	5
3	9999,0	21	6
4	0,00	0	0
5	0,00	0	0
6	0,00	0	0

PROFILE 4
(hot metal weight is up to 90 t)

Bucket 1

Ntap	Wsp	Ntr	Noc
1	15,00	15	1
2	25,00	16	2
3	35,00	17	3
4	9999,0	18	4
5	0,00	0	0
6	0,00	0	0

Bucket 2

Ntap	Wsp	Ntr	Noc
1	30,00	15	1
2	50,00	17	2
3	70,00	18	3
4	9999,0	18	4
5	0,00	0	0
6	0,00	0	0

Bucket 3

Ntap	Wsp	Ntr	Noc
1	30,00	15	1
2	50,00	17	2
3	70,00	18	3
4	9999,0	18	4
5	0,00	0	0
6	0,00	0	0

Steel refining

Ntap	Wsp	Ntr	Noc
1	80,00	18	4
2	9999,0	18	5
3	0,00	0	0
4	0,00	0	0
5	0,00	0	0
6	0,00	0	0

Setting Ntr, Noc and t_{PT} during re-arcing after deactivating EAF (refining stage)

Ntr 15 Noc 1 t_{PT}, c 10

Fig. 5. Melting profiles 3, 4 for the algorithm applied to automatically change on-load taps of the furnace transformer and operating curves

metal, but charging two additional buckets. In this case, $N_{TR} \leq 18$ is used, as in case with profile 4, which is required to limit heat impact of electric arcs on the EAF refractory lining, to achieve its optimal heating.

For clarity, oscillograms of the new algorithm applied to automatically change on-load taps of the furnace transformer and operating curves for profile 3 are given in **Fig. 6** (hot metal weight is 60 t, charge weight is 80 t).

In addition to the new algorithm, to enhance efficiency of manual control in the injection of the carbon-containing material and the correction of N_{TR} and N_{OPCURV} during operation of arcs on the molten bath to efficiently shield them and additionally increase thermal efficiency by the carbon injectors at the steel refining stage in the EAF, we introduced the steelmaker's visualization of the current value of slag foaming coefficient K_{SLAG} calculated by the formulae [12–15]:

$$K_I = \frac{\sqrt{I^2 - I_{(1)}^2 - I_{(0)}^2}}{I_{(1)}} \cdot 100\% = \frac{I_{HG}}{I_{(1)}} \cdot 100\% \quad (5),$$

$$K_{SLAG} = \frac{A}{K_{SLAG}} \cdot 100\% \quad (6)$$

where K_I is total harmonic distortion (THD_I), I is an actual (root mean square) value of current; $I_{(1)}$ is an actual value of the first harmonic current; $I_{(0)}$ is a constant component of current; I_{HG} is an actual value of higher harmonics, A is a scale coefficient.

The algorithm also includes the developed and studied approach to automatic control of RCBs and carbon injectors. Its main idea is as follows: having analyzed a large number of heats, we made a conclusion that when the furnace bath reaches a state close to complete melting of the solid charge, there is a sharp increase in K_{SLAG} due to active slag formation. This event serves as a criterion for switching RCBs from the burner mode to the lance mode. Then, as the carbon content in the melt decreases and slag is discharged through the relevant door, the arcs become exposed leading to a sharp decrease in K_{SLAG}. At this point, it is necessary to activate the carbon injectors and switch the lance to a reduced intensity mode to ensure melt stirring. A visual demonstration of the automatic operation of RCBs and injectors is shown in **Fig. 7**.

Based on implementing the stated measures in production and tests performed in pre-warranty and warranty periods and analyzing a large sample of heats, we noticed the significant technical effect, such as lower specific electrical energy consumption W_{SP}, from 231.6 kW·h/t to 203.0 kW·h/t, amounting to a 12.3 % decrease. This result is considerable for such energy-consuming equipment as the EAF and is expected to substantially reduce the final product's cost. It should be noted that the developed measured are universal and can be applied on other modular-type EAFs of different capacities.

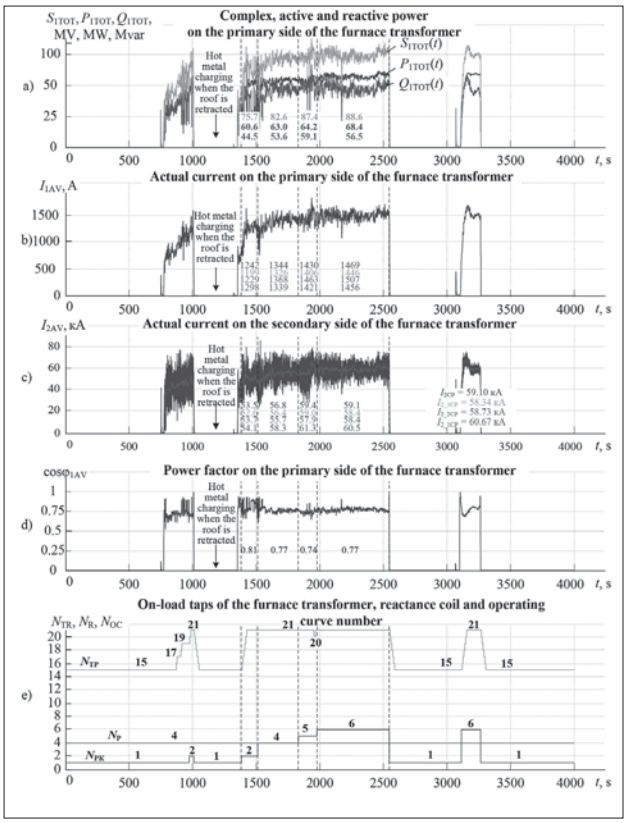

Fig. 6. Test melting at the most frequently used melting profile Hot metal $G_{HOTMETAL}$ = 60 t, charge G_{CHARGE} = 80 t, power-on time t_{PT} = 26.4 min, W_{SP} = 215 k·Wh/t

Conclusion

1. The EAF operation revealed the problems influencing energy efficiency: 1) non-optimal parameters of the HI-REG automatic control system for the electrical mode result in complex conductivity being controlled with a significant static error and slowed transfer processes of control actions; 2) manual control of the EAF electrical modes, changing the on-load tap of the furnace transformer and operating curve number by visually controlling the charge melting process.

2. To deal with the identified issues, the measures were taken to increase energy efficiency of the EAF. The first measure involved adjusting the automatic control system parameters for the electrical mode and electrode movement to decrease a static error of control and improve dynamic parameters of the control quality. The second measure was aimed at introducing the algorithm for automatic switching of furnace transformer taps and operating curves using individual melting profiles for various combinations of weight of the solid charge and hot metal.

3. We suggested and implemented a new approach to automatic control of RCBs and carbon injectors, whose main idea is based on the fact that when the furnace bath reaches the state close to complete melting of the solid charge, K_{SLAG} sharply increases due to active slag forming. This event serves as a criterion for switching the RCB from a burning mode to a blowing mode. Later, as the carbon content in the molten bath decreases, and slag is discharged through the door, the arcs are exposed, causing K_{SLAG} to decrease.

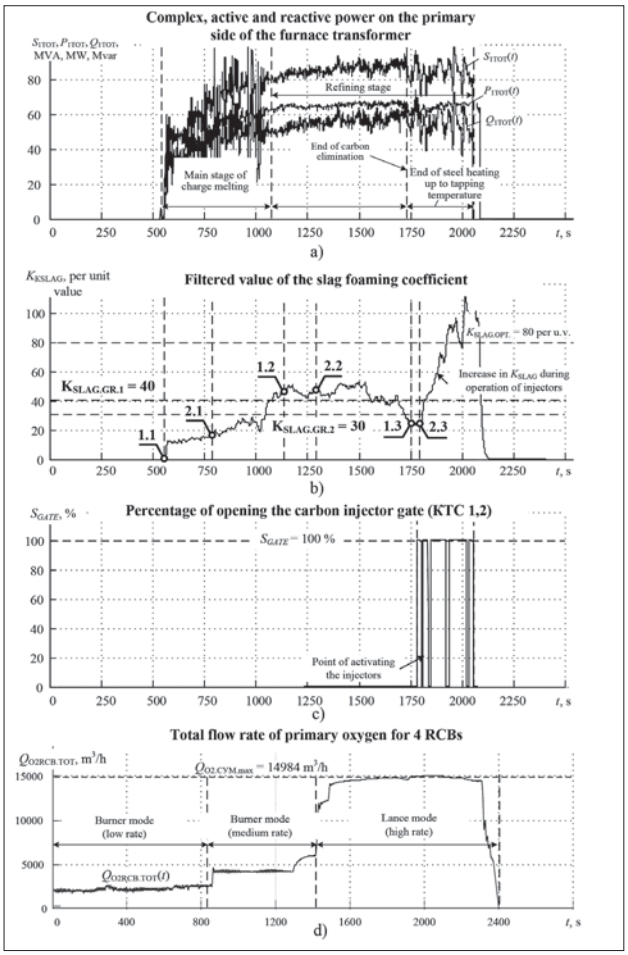

Fig.7. Time behavior of typical melting in the EAF (95 MVA): total complex, active and reactive power S_{1TOT}, P_{1TOT}, Q_{1TOT} (*a*); a filtered value of slag coeffi-cient K_{SLAG} with T_F =30 s (*b*); percentage of opening the carbon injector gate S_{GATE} (*c*); total oxy-gen flow rate for 4 RCBs $Q_{O2.TOT}$ (*d*)

In this case, an operator needs to activate carbon injectors and switch the lance to a lower rate mode to ensure proper mixing of the molten bath.

4. Upon implementation of the described measures and reviewing the results of the tests conducted in pre-warranty and warranty periods, and analysis of a large sample of heats, we observed the technical effect, namely lower specific electrical energy consumption WSP, decreasing from 231.6 kW·h/t to 203.0 kW·h/t, amounting to 12.3 %. The achieved result confirms that the approaches applied in the research are correct and reasonable. It is significant for the EAF as it contributes to a decrease in the final product's cost.

The research was funded by the Ministry of Science and Higher Education of the Russian Federation (project No. FZRU-2023-0008)

REFERENCES

1. Mironov Yu. M. Electric arc in electrotechnological installations: monograph. Cheboksary: Izdatelstvo Chuvashskogo Universiteta, 2013. 290 p.

2. Makarov A. N. Heat exchange laws between electric arc and flame in metallurgical furnaces and electric power facilities. Tver: Izdatelstvo Tverskogo Gosudarstvennogo Tekhnicheskogo Universiteta, 2012. 164 p.
3. Nekhamin S. M. Creation and implementation of energy-efficient arc and slag electric furnace complexes using direct current and low-frequency current: Dissertation ... of Doctor of Engineering Sciences. Moskovskiy energeticheskiy institut, Moscow. 2015.
4. Svenchanskiy A. D., Zherdev I. T., Kruchinin A. M. et al. Electrical industrial furnaces: arc furnaces and special heating installations: textbook for universities. Edited by A. D. Svenchanskiy. Moscow: Energoizdat, 1981. 296 p.
5. Mironov Yu. M. Regularities of electrical modes of arc steel-making furnaces. *Elektrichestvo*. 2006. No. 6. pp. 56–62.
6. Tuluevskiy Yu. N., Zinurov I. Yu. Innovations for electric arc furnaces. Scientific bases of choice: monograph. Novosibirsk: Izdatelstvo NGTU. 2010. Vol. 12. 347 p.
7. Babaei Z., Samet H. Three-phase Cassie arc equations for electric arc furnace. *IEEE Transactions on Plasma Science*. 2025. Vol. 53, No. 6. pp. 1299–1311. DOI: 10.1109/TPS.2025.3559717.
8. Babaei Z., Samet H. Vector polynomial electric arc furnace models. *IEEE Transactions on Power Delivery*. 2025. Vol. 40, No. 3. pp. 1694–1705.
9. Klimas M., Grabowski D. Application of the Deterministic Chaos in AC Electric Arc Furnace Modeling. *IEEE Transactions on Industry Applications*. 2024. Vol. 60, No. 3. pp. 4978–4986.
10. Nikolaev A. A., Tulupov P. G., Ryzhevol S. S. Development of an improved automatic control algorithm for combined RCB burners and carbonaceous material injectors of a flexible modular furnace. *Chernye Metally*. 2022. No. 10. pp. 67–72.
11. Nikolaev A. A., Tulupov P. G., Ryzhevol S. S. Optimal Adjustment Methodology for the Electric Mode Control System Non-Linear Regulator of Electric Arc Furnace. *2022 International Conference on Industrial Engineering, Applications and Manufacturing (ICIEAM): Proceedings*. Sochi, Russian Federation, 2022. pp. 712–716.
12. Jansen T., Krüger K., Schliephake H. et al. Advanced foaming slag control. *The 10th European Electric Steelmaking Conference: Proceedings*. Graz, 2012. September 25–28.
13. Jansen T., Krüger K., Schliephake H. et al. DC-EAF power control using a sound based foaming slag signal. *Chernye Metally*. 2011. No. 2. pp. 20–25.
14. Nikolaev A. A., Tulupov P. G., Anufriev A. V. Assessing the feasibility of electrical mode control of ultra-high power arc steelmaking furnace based on data about harmonic composition of arc currents and voltages. *Research and Education in Mechatronics (REM): Proceedings of the 16th International Conference*. Bochum, Germany. 2015. pp. 301–308.
15. Nikolaev A. A., Bulanov M. V., Tulupov P. G., Ivekeev V. S., Ryzhevol S. S., Afanasev M. Iu. Optimizing time, power and technolo-gical parameters of modular-type electric arc furnaces: monograph. Magnitogorsk: Izdatelstvo MGTU im. G. I. Nosova, 2024. 419 p.